

Improvement of Microfiltration Performance by Critical Flux in Water Treatment

Dae-Young Kwon
Department of Environmental Engineering & Biotechnology

수처리시 임계 플럭스에 의한 막여과 효율 증대

권대영
명지대학교, 환경생물공학과

1. Introduction

One of the major drawbacks hindering the application of membrane processes in water and wastewater treatment is the reduction in the flux with time (below the theoretical capacity of the membrane). Under the conditions of constant transmembrane pressure (TMP) and cross-flow velocity, the flux in cross-flow microfiltration (CFMF) declines to a steady-state value which can be as much as two orders of magnitude lower than the initial or clean water value (Lokjin et al., 1992). In general, the typical temporary variation of the flux is an initial rapid decrease followed by a long but slow and gradual flux decline till it reaches the steady-state flux.

It is well known that membrane fouling is one of the main phenomena responsible for this flux decline. The fouling mechanism is extremely complicated. The fouling affects the performance of the membrane either by deposition of a layer onto the membrane surface or, by complete or partial blockage of the membrane pores. This changes the effective membrane pore size distribution (Tarleton et al., 1993).

In this study, a critical flux was defined based on TMP increase, below which the CFMF can be operated without membrane fouling. From CFMF experiments under constant permeate flux operational mode, the factors (such as particle size, membrane pore size, cross-flow velocity) affecting these critical flux values are discussed. The hydrodynamic force balance model was also developed to calculate the critical flux.

2. Experimental

The schematic diagram of the CFMF set-up used in this work is shown in Figure 1. Monodispersed suspension of spherical polystyrene latex particles (of pre-determined concentration) was delivered from a stock tank (equipped with a stirrer) to the CFMF cell by a variable speed tubing pump. Both the permeate and retentate lines were returned to the stock tank to maintain constant inlet concentration. The pressure of membrane was controlled by two valves (as shown in Figure 1) and the transmembrane pressure drop was monitored by using a pressure transducers (Model 19-626A from Devar Inc.) at three points (P_1 , P_2 and P_3) every two minutes. The permeate flux was kept constant for 20 (to almost 50 minutes in some cases) by the suction pump (Watson Marlow 505S), the speed of which can be changed.

The dimensions of the filtration channel in the CFMF cell are 6cm, 0.6cm and 0.036cm of length, width and thickness respectively. The CFMF cell has 9 filtration channels and the total membrane area is $3.24 \times 10^{-3} \text{m}^2$. The solution was circulated (crossflow filtration) along the surface of the flat-plate membrane in the module in which the cells are

sufficiently spaced. Thus, one could consider that they do not interfere to each other from mass transfer or hydrodynamic point of view. The membranes used are PVDF (polyvinyl fluoride) membrane (MILLIPORE : Catalogue no. GVLP OMS 10) with nominal pore size of $0.2\mu\text{m}$. In each experiment, new membrane was used to obtain reproducible results.

Different sizes of polystyrene latex particles ($0.3\mu\text{m}$, $0.46\mu\text{m}$, $0.816\mu\text{m}$, $1.07\mu\text{m}$, $3.2\mu\text{m}$ and $11.9\mu\text{m}$ in diameter) were used in this study. They all were larger than the membrane pore size to prevent particles from penetrating into the membrane pores. Influent concentration was monitored in terms of the turbidity of suspension in the feed tank. The turbidity of suspension was measured using a turbidimeter (2100P TURBIDIMETER, HACH). The standard deviation in particle size was less than 10% and their specific density was 1.05g/cm^3 . A feed solution was prepared by adding a known amount of latex particles. The temperature was the ambient temperature ($25\pm 2^\circ\text{C}$) and the pH was kept as 6 ± 0.5 by adding HCl or NaOH in each experiment

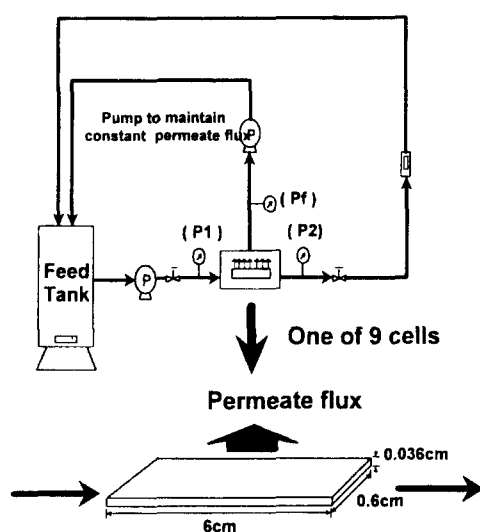


Figure 1. CFMF experimental set-up

3. Definition of critical flux

The concept of critical flux has been recently introduced with a number of theoretical and experimental evidences. The concept of critical flux proposed by Field et al (1995) and Howell (1995) states that *“on start-up there exists a flux below which a decline of flux with time does not occur : above it fouling is observed. This flux is the critical flux and its value depends on the hydrodynamics and probably also on the other variables”*. This flux should be equivalent to the corresponding clean water flux at the same TMP. Theoretical calculations for particles of different sizes made by Bacchin et al (1995) suggested that different mechanisms govern the critical flux of different sizes of particles. For small particles of the order of $0.1\mu\text{m}$, Stoke-Einstein diffusion away from the membrane surface is important and the critical flux depends

significantly on the surface charge effects. For particles over $1 \mu\text{m}$, they are lifted from the surface by the shear-induced diffusion and the surface charge has insignificant effect. The operation of CFMF below critical flux may provide a significant technical and economical advantage. If it is sustained, the cost of membrane cleaning can be removed and the life span of membrane can be prolonged significantly. Furthermore, a benefit of CFMF below critical flux over normal CFMF in terms of water quantity can be seen in Figure 1.

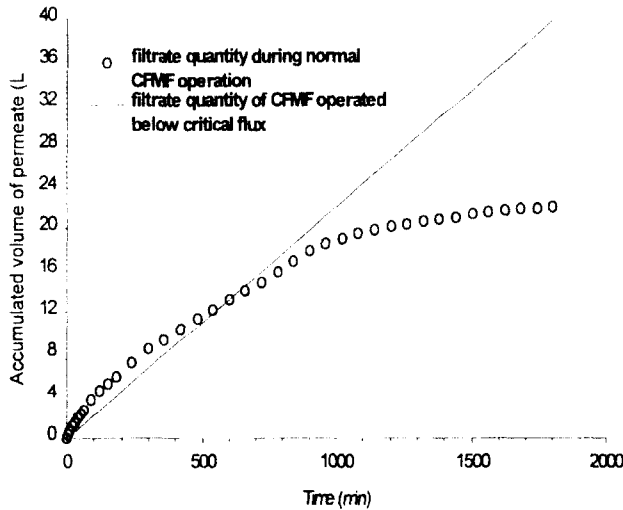


Figure 2. Comparison of total permeate volumes from CFMFs at constant pressure and below critical flux (particles size of $0.46 \mu\text{m}$, membrane pore size of $0.2 \mu\text{m}$ and influent concentration of 40mg/L)

In this figure, volume of permeate from CFMF below critical flux was calculated on the basis of the critical flux value ($410 \text{ L/m}^2\text{h}$) which was obtained from the experiment under the identical condition. As can be seen in the figure, the accumulated volume of permeate from CFMF below critical flux exceeded that from normal CFMF after 600 minutes.

4. Force balance model

Figure 3 illustrates the forces acting upon a particle located in the polarised layer. As shown in the figure, there are three main forces; a net tangential force (F_x), a net normal force (F_y) and a interparticle force (F_{ip}). Each of them can be simply described as follows.

The tangential force exerted on a single particle touching a plane surface in a uniform velocity gradient has been evaluated by O'Neil (1968);

$$F_x = 1.7009(3\pi)\mu d_p u_x \text{ (at } z = d_p / 2) \quad (1)$$

Note that u_x is the fluid velocity at the position of particle center when particle is absent, and 1.7009 is the wall correction factor of Stokes' law derived by O'Neil.

The normal force is the summation of normal drag force produced by the permeate flow and back transport force;

$$F_y = F_n - F_{ht} \quad (2)$$

Goren (1979) solved the resisting drag of a spherical particle with uniform velocity U_∞ approaching a permeable wall, and he concluded that for a finite value of wall permeability, a

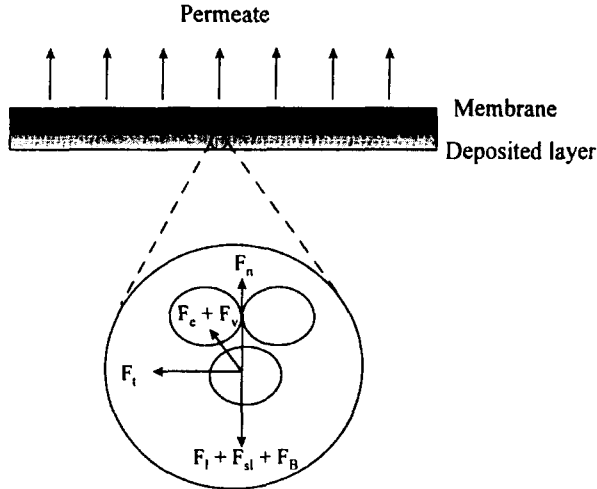


Figure 3. Schematic representation of forces exerted on the particle in the deposited layer

finite hydrodynamic force on the particle was expected even for the particle touching the wall. When the particle and wall were in contact, he derived the drag force as ;

$$F = 3\pi\mu d_p u_\infty \phi \quad (3)$$

where, ϕ is the wall correction factor of Stokes' law for the corresponding flow system.

As a result, the normal drag force supporting a particle remaining on the polarised layer can be obtained by replacing U_∞ with the permeate flow u_p in the equation (4), i.e.,

$$F_n = 3\pi\mu d_p u_p \phi \quad (4)$$

Similarly, the transport force can be expressed as ;

$$F_{bt} = 3\pi\mu d_p u_{bt} \phi \quad (5)$$

where, the back transport velocity, u_{bt} , consists of the lateral migration velocity, u_l , the shear induced velocity, u_s , and Brownian diffusion velocity, u_B , which are available in the literature (Wiesner et al., 1989 and Drew et al., 1991) ;

The interparticle force can be described by the summation of double layer repulsive and van der waals attractive forces ;

$$F_{ip} = F_{DL} - F_{VDW} \quad (6)$$

(i) Double layer repulsive force

In aqueous suspensions, the electrostatic force is due to the formation of Debye-Huckel double layers at the particles. Hogg et al (1966) proposed that the double layer repulsive force, FDL, between the particles with approximately equal potential, ϕ , is ;

$$F_{DL} = \frac{\pi \epsilon_c \epsilon_0 \phi^2 d_p \kappa \exp(-\kappa h)}{1 - \exp(-\kappa h)} \quad (7)$$

where, ϵ_c is the dielectric constant of fluid, ϵ_0 is the permittivity of a vacuum and κ is the Debye reciprocal length.

(ii) Van der Waals attractive force

Hamaker (1937) has shown that the unretarded van der waals attractive force between particles is ;

$$F_{vdw} = \frac{H}{12d_p} \left(\frac{2d_p}{h} - \frac{d_p^2}{h^2} - \frac{2d_p}{h+d_p} - \frac{d_p^2}{(h+d_p)^2} \right) \quad (8)$$

where, the Hamaker constant, H, depends on the nature of the particle and the intervening fluid. As shown in Figure 1, the moment of all forces about the contact point G can be calculated as ;

$$M = \frac{d_p}{2} \left\{ F_x \sin\theta - [F_y + k_f F_p] \cos\theta \right\} \quad (9)$$

The sign of the net moment calculated from the equation (9) will determine whether or not the deposited layer will be accumulated by the additional deposition. A positive value of the net moment shows that the particle will be swept off the layer, and a negative value shows that the layer will develop to the cake formation resulting in the increase of membrane resistance. A critical state is reached when the forces on the particle are balance or in equilibrium, at which the net moment is equal zero.

5. Experimental method to define critical flux

The following equation can be used to describe the overall characteristics of flux decline (Aimar et al., 1989).

$$J = \frac{\Delta P}{\mu(R_m + R_f)} \quad (10)$$

where, J is the permeate flux (permeate flow per unit membrane area), ΔP is TMP, μ is the viscosity and R_m is the clean membrane hydraulic resistance. The resistance, R_f accounts for the fouling effects on the flux. From this equation, it is evident that R_f is dependent only on the TMP if the CFMF is operated at a constant permeate flux. Thus, there will be no increase in the TMP with time if no or negligible membrane fouling occurs at a given constant flux. However, the TMP will increase with time if the flux is increased beyond a certain value. In other words, the membrane fouling can be detected in terms of the increase in the TMP.

6. Result and discussion

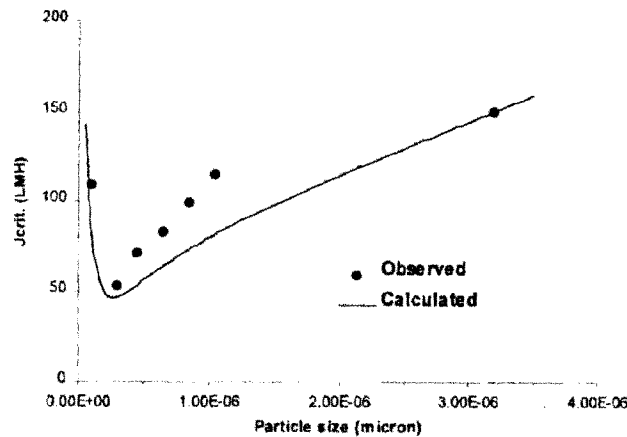


Figure 4. Effect of particle size on critical flux (membrane pore size of 0.1 μm, influent concentration of 200mg/L and cross-flow velocity of 0.2m/s)

Effect of particle size

A series of experiments were conducted to study the effect of particle size on critical flux. Different sizes of latex particles (0.1, 0.3, 0.46, 0.816, 1.07 and 3.2 μm) were used in the experiments. The other experimental conditions were maintained constant. In each experiment, the permeate flux was increased step by step until an increase of TMP with time was observed. Figure 4 presents the critical flux values for different sizes of latex particles used. The maximum flux corresponding to no increase in TMP with time and the minimum flux which resulted in TMP increase in time were noted. The average of these two values is taken as critical flux.

It can be seen from the figure that the critical flux increased with the increase in the particle size. This might be due to the fact that the smaller particles have preferential tendency of deposition on the membrane at lower permeate flux. However, one should keep in mind the fact that the increase of TMP with time was a crucial point to define a critical flux in Figure 4. As discussed earlier, the TMP increase depends only on the fouling resistance at a constant permeate flux operational mode. Therefore, the different critical flux value with different particle size is due to the variation in the resistance of the deposited particles to flux. Note in this figure that the critical flux can be predicted accurately by the model developed in this study.

Effect of membrane pore size

Figure 5 presents the critical flux obtained from the experiments with membranes of different pore sizes (0.1 μm , 0.2 μm , 0.45 μm and 0.65 μm). For the experimental conditions studied, the membrane pore size did not have significant effect on critical flux. The result is perhaps surprising when one takes into account the difference in the intrinsic resistance of the four membranes (see Table 1). Table 1 shows that the difference in the magnitude of the resistance value of membranes of 0.1 μm and 0.65 μm is approximately two order. However, the permeate flux was maintained constant in these experiments. Same values of the critical flux for the different pore sizes of membranes indicate that the drag force to capture the particle onto the membrane surface is identical irrespective of the different pore size of the membranes (0.1 to 0.65 μm).

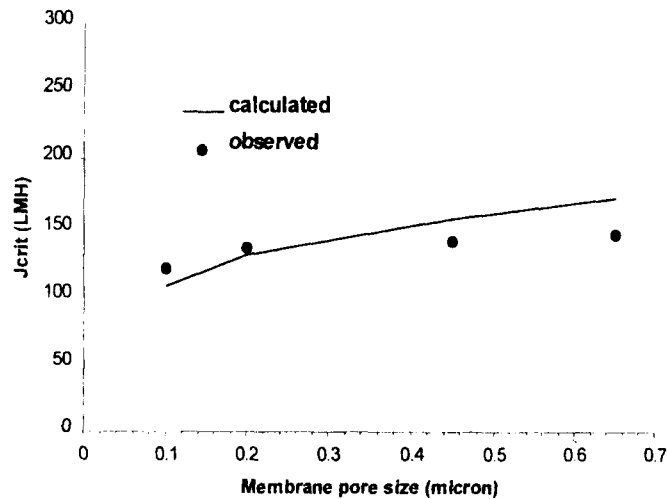


Figure 5. Effect of membrane pore size on critical flux (particle size of 0.816 μm , influent concentration of 100mg/L and cross-flow velocity of 0.2m/s)

Table 1. Intrinsic resistance of membrane

Membrane pore size (μm)	Resistance ($1/\text{m}$)
0.1	1.04×10^{11}
0.2	3.0×10^{10}
0.45	7.2×10^9
0.65	4.3×10^9

Effect of cross-flow velocity

The influence of cross-flow velocity on the critical flux is shown in Figure 6. As can be seen from the figure, the critical flux increased with the increase in cross-flow velocity. Several experimental data (Dahlheimer et al., 1970, Baker et al., 1985 and Lu et al., 1989) showed that a higher cross-flow velocity always induces a thinner cake formation, thus resulting in a lower hydraulic resistance. Fischer and Raasch (1986) also claimed that the tangential drag force due to cross-flow is proportional to the shear stress at the wall, τ_w ; and, the normal drag force due to permeation flow is proportional to the permeate flux, q . They also found that the critical selective cut-diameter of the deposited particle is proportional to q/τ_w , which explains why the higher cross-flow velocity forms a thinner particle cake on the membrane surface during the CFMF operation. It might also be due to the fact that the migration force, which causes the sweep of the deposited particles away from the surface, would be stronger at higher cross-flow velocity.

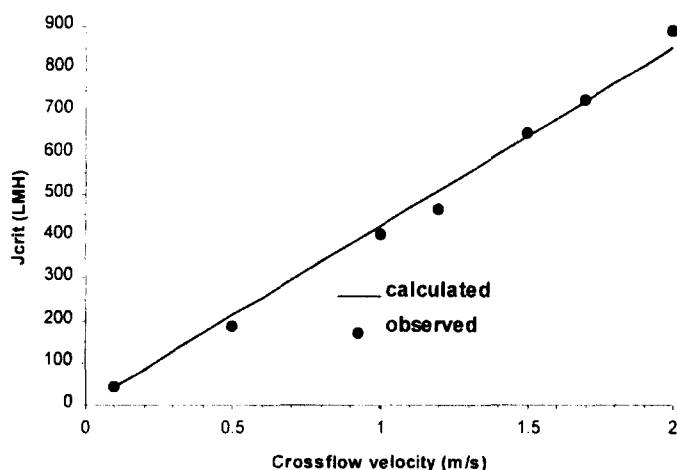


Figure 6. Effect of cross-flow velocity on critical flux (particles size of $0.46\mu\text{m}$, membrane pore size of $0.2\mu\text{m}$ and influent concentration of 10mg/L)

7. Conclusions

A laboratory - scale experimental study has been conducted to investigate the effect of different parameters on membrane fouling in CFMF and the following observations were made :

- At high applied pressure (80 or 100 kPa), the initial flux was higher, but the final flux (at 120 minutes) was approximately same as that at 40 kPa. The flux at low applied pressure (5 or 10 kPa) maintained constant throughout the filter run.
- The higher the cross-flow velocity, the less the flux reduction with time.

- Membrane pore size had insignificant effect on the final flux (after 180 minutes) although the initial flux of the membrane of bigger pore was greater than that of the smaller pore. The critical flux was defined as a flux below which no flux decline occurs with operation. The advantage of the CFMF below critical flux was also presented. From the experiments to study the effects of particle size, membrane pore size, cross-flow velocity, on the critical flux, the followings were concluded :
 - The smaller the particle, the lower the critical flux (for a size range of 0.32 ~ 3.2 μm).
 - Similar value of critical flux was obtained for different pore size of membranes (0.1, 0.2, 0.45 and 0.65 μm in pore size). However, above the critical flux, the fouling of the membrane with bigger pore size was more significant than that with smaller pore size.
 - The higher the cross-flow velocity, the greater the critical flux.

8. References

1. Aimar, P. and Howell, J. A., (1989) Effects of concentration boundary layer development on the flux limitations in ultrafiltration, *Chem. Eng. Res. Des.*, 67, 255-261
2. Baker, R. J., Fane, A. J., Fell, C. J. D. and Yoo, B. H., (1985) Factors affecting flux in crossflow filtration, *Desalination*, 53, 81
3. Bacchin, P., Aimar, P. and Sanchez, V., (1995) Model for colloidal fouling of membranes, *AICHE J.*, Vol 41, No2, 368-376
4. Carman, P. C. (1938) Fundamental principles of industrial filtration, *Trans, Inst. Chem. Eng.* 16, 168-187.
5. Dahlheimer, J. A., Thoas, D. G. and Kraus, K. A., (1970) Hyperfiltration : Application of woven fiber hoses to hyperfiltration of salts and crossflow filtrations of suspended solids, *Ind. Eng. Chem., Process Des. Dev.*, 4, 9
6. Fane, A.G., (1984) Ultrafiltration of dispersions. *J. Mem. Sci.*, 20, 249-259
7. Field, R. W. Wu, D., Howell, J. A. and Gupta, B. B., (1995) Critical flux concept for microfiltration fouling, *J. Mem. Sci.*, 100, 259-272
8. Fischer, E. and Raasch, J., (1986) Model tests of the particle deposition at the filter medium in cross-flow filtration, *Proc 4th World Filtration Congress*, 11.11-11.17, (KVIV, Ostend, Belgium)
9. Howell, J. A., (1995) Sub-critical flux operation of microfiltration *J. Mem. Sci.*, 107, 165-171
10. Lokjine, M. H., Field, R. W. and Howell, J. A., (1992) Crossflow filtration of cell suspensions : A review of models with emphasis on particle size effects, *Trans I Chem E*, 70, Part C: 149
11. Lu, W. M. and Ju, S. C., (1989) Selective particle deposition in crossflow filtration, *Sep. Sci. & Tech.*, 24, 517-540
12. Tarleton, E.S. and Wakeman, R.J., (1993) Understanding flux decline in crossflow microfiltration - Part 3 : Effects of membrane morphology, *Trans I Chem E*, 71, Part A : 521